LrhA promotes CRISPR-Cas immunity by enhancing primed adaptation in *Escherichia coli*

Mengdie Fang [1,2], Na Li [1], Mengxin Gong [1], Mingyue Fei [1], Yalan Lu [1], Mingjing Yu [1], Fabai Wu [3], Dongchang Sun [1]*

[1] College of Biotechnology and Bioengineering, Zhejiang University of Technology, Hangzhou, Zhejiang, 310014, China
[2] School of Laboratory Medicine and Bioengineering, Hangzhou Medical College, Hangzhou, Zhejiang, 310013, China
[3] School of Life Sciences, College of Science, Eastern Institute of Technology, Ningbo, China
*Corresponding author(s): Dongchang Sun

Email: sundch@zjut.edu.cn
Tel/Fax: +86 0571 88320057

Author Contributions: M.Fang, F. W. and D.S. conceived the study; M.Fang, N.L., M.G., M.Fei, Y.L., M.Y., F. W. and D.S. designed research; M.Fang, N.L., M.G., M.Fei, Y.L., and M.Y., performed research; M.Fang, N.L., M.G., M.Fei, Y.L., M.Y., and D.S. analyzed data; and M.Fang., and D.S. wrote the paper.

Competing Interest Statement: We declare that we have no financial and personal relationships with other people or organizations that can inappropriately influence our work, there is no professional or other personal interest of any nature or kind in any product, service and/or company that could be construed as influencing the position presented in, or the review of, the manuscript entitled.

Keywords: Adaptive immunity | LrhA | CRISPR interference | CRISPR adaptation | Transcriptional regulator

ABSTRACT

The CRISPR-based defense system protects prokaryotes against foreign genetic elements. Previous studies indicated that the activity of the CRISPR-Cas system is the outcome of the combined effect of adaptation and interference. However, it remains unclear how coordination of the two processes is regulated to optimize the efficacy of adaptive immunity. Here, we identify the LysR-type transcriptional regulator LrhA as a new CRISPR-Cas activator which plays an important role in coordinating adaptation and interference. Through directly binding to the promoter of the *cas* operon, LrhA enhances the CRISPR-Cas adaptive immunity against bacteriophage infection by stimulating the transcription of *cas* genes. Moderate activation of *cas* genes by LrhA efficiently promoted the clearance of horizontally transferred CRISPR-targeted plasmid via increasing the acquisition of new spacers by interference-driven adaptation in *Escherichia coli*. Our results indicate that intermediate level of transcription of *cas* genes achieved optimal outcomes of the adaptive immunity through triggering positive feedback between adaptation and interference, highlighting the importance of fine-tuning expression of CRISPR-Cas system.

52 **INTRODUCTION**

53 Prokaryotes have evolved diverse defense systems against plasmids and viruses [1, 2, 3, 4].
54 Among them, the CRISPR-Cas adaptive immune system provides bacteria and archaea
55 with acquired and inheritable immunity against previously encountered invading nucleic
56 acids[5, 6, 7, 8, 9, 10]. The CRISPR-Cas system acts in three distinct stages. During the first
57 contact with a foreign genetic element, short DNA fragments from this element are
58 incorporated into the CRISPR array, which contains the genetic memory of previously
59 infecting elements[11, 12, 13]. The incorporation of a new spacer derived from the foreign DNA
60 leads to the expansion of the size of the CRISPR array. This process is termed adaptation[14,
61 15, 16, 17]. Under certain conditions, Cas proteins are expressed, accompanied by the
62 transcription of the CRISPR array, and subsequent processing of the premature CRISPR
63 RNA (pre-crRNA) into mature crRNAs[18, 19]. In the final stage termed interference, crRNAs
64 guide Cas proteins to the target sequence, where the Cas effectors are recruited for cleaving
65 the previously encountered foreign DNA[20, 21]. Native CRISPR-Cas systems have been
66 engineered for broad applications such as genome editing tools[22, 23, 24, 25] and antimicrobials
67 for combating multi-drug resistant (MDR) bacteria [26, 27, 28, 29, 30, 31].
68 CRISPR-Cas adaptive immunity represents a powerful weapon of defense in prokaryotes.
69 On the other hand, invasive nucleic acids often rapidly evolve resistance to CRISPR
70 immunity by mutating the CRISPR-targeted region. To fight back, a process named
71 'primed adaptation' is provoked to rapidly incorporate new spacers, derived from DNA
72 fragments produced by interference, for upgrading the CRISPR-Cas adaptive immunity[32,
73 33, 34]. Primed adaptation requires components for assembly of the interference and the
74 adaptation complexes[32, 35]. Nevertheless, a chronic high-level of CRISPR-Cas adaptive
75 immunity increases the burden of producing Cas proteins and crRNAs, as well as the risk
76 of suicide from autoimmunity[36, 37, 38, 39]. To finely tune the CRISPR immunity to a moderate
77 level, interference and adaptation are often inversely correlated: an intermediate level of
78 interference allows invasive nucleic acids to persist longer, leading to higher levels of
79 adaptation (interference-driven adaptation), while a strong interference leads to a relatively
80 low level of adaptation [40, 41]. Although the working mechanisms of CRISPR adaptation and
81 interference have been intensively investigated[11, 14, 16, 17, 35, 42, 43, 44, 45, 46, 47, 48], little is known
82 about how the CRISPR-Cas adaptive immunity is adjusted by leveraging both CRISPR
83 interference and adaptation, when facing different types of vulnerabilities [18, 19].
84 The type I CRISPR-Cas system, comprised of the multi-subunit RNA-guided surveillance
85 complex Cascade, the Cas3 nuclease, and the Cas1-Cas2 integrase, is most prevalent in
86 prokaryotes[49]. Regulation studies have focused on type I CRISPR-Cas systems [18, 40, 50, 51,
87 52, 53, 54, 55, 56, 57, 58, 59], especially the type I-E CRISPR-Cas system of *Escherichia coli*, in
88 which CRISPR interference is regulated by the LysR type transcriptional regulator (LTTR)
89 LeuO [60, 61], the histone-like proteins H-NS and StpA [62, 63, 64], and the carbon catabolite
90 regulator CRP[65]. Nevertheless, regulation of CRISPR adaptation has rarely been
91 investigated in *E. coli*. Less is known about how CRISPR adaptation and interference are
92 coordinated. We hypothesized the presence of host factor(s) that are involved in the
93 coordination of CRISPR adaptation and interference, and effectively aid the bacteria to
94 counter foreign DNA under certain scenarios.
95 To search for host factor(s) that control the adaptive immunity through coordinating
96 CRISPR adaptation and interference in *E. coli*, we screened for new regulators involved in
97 regulating transcription of *cas* genes by combining DNA pull-down and mass spectrometry,

98 and identified the LTTR protein LrhA as an important activator, which directly bound to
99 the promoter of the *cas* operon, and stimulated the CRISPR-Cas adaptive immunity against
100 bacteriophage infection. By promoting a positive feedback circuit between interference and
101 adaptation, LrhA remarkably augmented the clearance of CRISPR-targeted plasmid, via
102 moderately stimulating the transcription of *cas* genes required for both adaptation and
103 interference. Our work uncovers that intermediate level of transcription of *cas* genes
104 enables coordination of interference and adaptation to achieve optimal adaptive immunity,
105 gaining new insights into the regulation of bacterial defence against horizontally
106 transferred plasmids.

107 # RESULTS

108 ## Screening for proteins binding to the promoter of *cas* genes

109 Expression of the *cas* operon is regulated by H-NS and LeuO, which bind to specific sites
110 within P_{cas} [60, 62] (Fig. 1a, Fig. S1). To screen for new regulators that potentially affect the
111 transcription of *cas* genes, we performed a DNA pull-down assay using a DNA probe
112 containing P_{cas} as a bait (Fig. 1a). Because H-NS binds to high-affinity sites within P_{cas} and
113 possibly spreads along the adjacent DNA[66], potentially masking the binding sites of other
114 regulators, we screened for proteins binding to P_{cas} in *hns*-deletion mutants of two *E. coli*
115 strains (MC4100 and BW25113). Mass spectrometry analysis showed that more than one
116 hundred proteins in each strain were isolated with the biotinylated P_{cas} (Fig. S2a). Among
117 them, 49 proteins were detected in both strains (Fig. S2b, Table S1). According to the
118 bioinformatic analysis of proteins with high coverage of matched peptides, 18 proteins
119 were classified as transcriptional factors (TFs) (Fig. 1b, Table S2). Two previously
120 documented regulators of the CRISPR-Cas system (i.e. StpA[63, 64] and SlyA[67]) were
121 identified in the protein mixture bound to P_{cas}, indicating that the screening approach was
122 effective.
123 Remarkably, the LTTR LrhA was highly abundant in protein mixtures bound to P_{cas} in both
124 strains (Fig. 1b and c), with high coverage of peptide sequences (Fig. S3). Subsequent pull-
125 down assay confirmed that purified LrhA with a 6×His-tag bound P_{cas}, indicating that LrhA
126 could be a potential regulator of the CRISPR-Cas system in *E. coli* (Fig. 1d).
127 To check whether these P_{cas}-binding TFs regulate transcription of the *cas* operon, their
128 effects on the activity of P_{cas} were evaluated with a previously described fluorescence
129 reporter system[64] (Fig. 1e). To avoid the effect of the known strong regulators H-NS and
130 LeuO, the 12 predicted TFs, and LeuO (as the positive control), were separately over-
131 expressed in a Δ*hns* Δ*leuO* mutant. SlyA promoted the activity of P_{cas} by 2.4-fold (Fig. 1e),
132 in agreement with the previous report [67]. Eight TFs contain the HTH-type DNA binding
133 domain, which is also present in LeuO (Fig. 1f). The LTTR ArgP, known to act either as a
134 transcriptional activator or a repressor depending on its binding with two effectors lysine
135 and arginine[68], reduced the activity of P_{cas} by 70%, while LrhA increased the activity of
136 P_{cas} by more than 2-fold (Fig. 1e). Although YdcI and AaeR also belong to LTTRs and
137 bind to P_{cas}, they showed minimal (if any) effect on the activity of P_{cas} (Fig. 1e). Thus, we
138 narrowed down to the regulators LrhA, SlyA, ArgP and HexR below. To investigate their
139 potential functions on regulating CRISPR interference, a conjugative plasmid pTc, that
140 carries a DNA fragment with four protospacer-adjacent motif (PAM)-containing spacers
141 from pT[64] , was generated. By examining clearance of the CRISPR-targeted plasmid (pTc)
142 and the CRISPR-non-targeted plasmid (pNTc) in the BW25113 Δ*hns* Δ*leuO* mutant during

conjugation. As shown in Fig. S4, LrhA and LeuO decreased the conjugation frequencies of pTc but not pNTc after 24h growth, exhibiting a higher CRISPR immunity than the Vector. ArgP did not affect the clearance rates of both plasmids significantly, with its CRISPR immunity unaffected. Overexpression of HexR or SlyA reduced plasmid stability, thus the conjugation frequencies of both plasmids were not detected (Fig. S4). Therefore, we focused on LrhA in the following investigation.

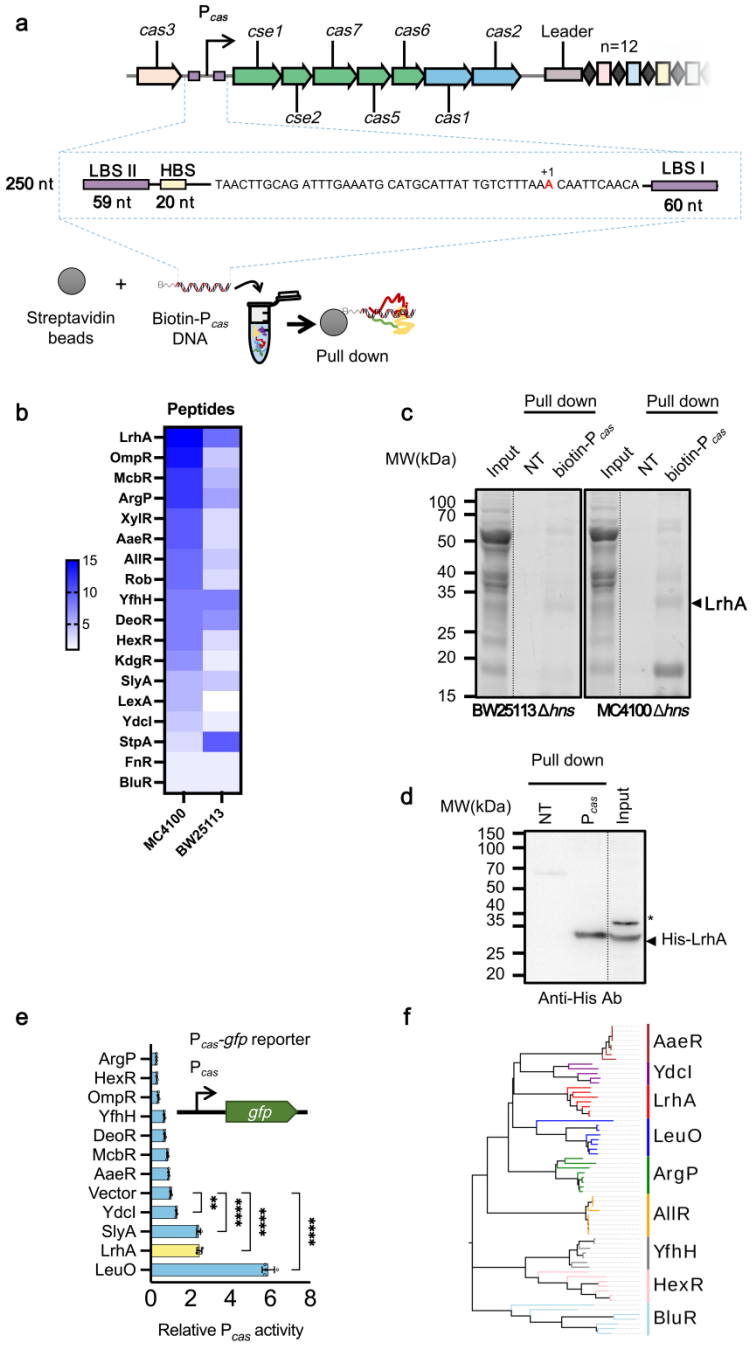

Figure 1. Screen for new regulators modulating transcription of *cas* genes. (**a**) Schematic illustration of the CRISPR-Cas locus in *E. coli*. Repeats (diamonds) in the CRISPR array are interspersed with 12 unique spacer sequences (rectangles). The promoter of the *cas* operon (P_{cas}) is indicated by the black arrow. The P_{cas} DNA probe for pull-down assay contains a transcription

start site (red letter), LeuO binding site I and II (LBS I/II; purple bars), and H-NS binding site (HBS; yellow bar). For the pull-down proteomic experiment, a biotinylated probe (biotin-P_{cas} DNA) was immobilized onto streptavidin beads, followed by incubation with extracts from *E. coli* MC4100 Δ*hns* (ZJUTCBB0015) or BW25113 Δ*hns* (ZJUTCBB0009) before SDS-PAGE electrophoresis. (**b**) A heatmap shows the number of peptides pulled down by P_{cas} DNA probe. (**c**) SDS-PAGE gel electrophoresis of nontargeted biocytin (negative control, NT) or biotin-P_{cas} DNA-binding proteins. NT or biotin-P_{cas} samples were digested in gel with trypsin, and corresponding peptides were analyzed by mass spectrometry. An arrow denotes the band corresponding to LrhA (34.593 kDa). (**d**) Pull-down assay of physical interaction between LrhA and P_{cas}. The biotinylated probe (biotin-P_{cas} DNA) was immobilized onto streptavidin beads and incubated with His-LrhA from cell extracts before (lane 3, input) and after (lane 2, P_{cas}) pull-down, followed by western blot assay with antibody against His-tag. Nontargeted biocytin (NT) was used as a negative control (lane 1). Arrow indicates the band of His-LrhA, and the asterisk indicates a non-specific band. (**e**) Effects of 12 predicted TFs and LeuO on the P_{cas} activity in *E. coli* BW25113 Δ*hns* Δ*leuO* (EC73). The expression of TFs was induced by adding 10 mM arabinose. The P_{cas} activity was evaluated by GFP/OD_{600} at 37 ℃, with the relative expression level of Δ*hns* Δ*leuO* carrying empty vector pSU19 (Vector) as 1 arbitrary unit. All bars represent the mean, and error bars denote standard deviation. Individual biological replicates are shown (n = 4). Statistical significance was determined using one-way ANOVA with Dunnett's multiple comparisons test. ****, $P < 0.0001$; **, $P < 0.01$ (**f**) Phylogenetic analysis of 9 HTH-type P_{cas}-binding TFs from 5-8 different bacteria species.

LrhA activates transcription of the *cas* operon by binding to P_{cas}

We investigated transcriptional regulation of P_{cas} in *E. coli* K12 BW25113, which has an active type I-E CRIPSR-Cas system[65] , and ER2738, an F^+ *E. coli* strain which is commonly used as a host strain for M13 phage amplification. ER2738 possesses not only intact *hns* and *leuO* genes (GenBank accession number PP194455, PP194456, PP112993), but also *cas* genes and CRISPR arrays, and their promoters (Fig. S5, GenBank accession number, PP194457), sequences of which are identical to that in BW25113. By using the P_{cas}-*gfp* reporter, we observed that the P_{cas} activity was 2.5-fold lower in ER2738 WT than in ER2738 Δ*hns*, while P_{cas} activity was 14.5-fold lower in BW25113 WT than in BW25113 Δ*hns* (Fig. 2a), indicating that the repression effect of H-NS on P_{cas} is remarkably weaker in ER2738 than in BW25113. qPCR analysis revealed that the amount of *hns* mRNA was more than 10-fold lower in ER2738 than in BW25113, indicating low expression of H-NS in the former strain (Fig. 2b). We inactivated *lrhA* in the Δ*hns* and Δ*hns* Δ*leuO* mutants to further evaluated how LrhA controls the transcription of the *cas* operon in both ER2738 and BW25113. In agreement with the previous report that LrhA represses transcription of the motility master regulator operon *flhDC*[69], deleting *lrhA* increased the diameter of swarm rings (Fig. S6), showing correct construction of these strains. We detected no significant effect of chromosomally expressed LrhA on the transcription of the first gene of the *cas* operon (i.e., *cse1*) in BW25113 WT (Fig. 2c), while transcription of *cse1* was 4.4-fold lower in ER2738 Δ*lrhA* than in ER2738 WT (Fig. 2d), indicating that LrhA displays stronger effect on P_{cas} in ER2738 than in BW25113. In the BW25113 Δ*hns* mutant, deleting *lrhA* decreased transcription of *cse1* by 11%. Further deleting *leuO* made LrhA exhibit a more pronounced effect on the activity of P_{cas}. Deleting *lrhA* decreased transcription of *cse1* by 26% in the BW25113 Δ*hns* Δ*leuO* mutant (Fig. 2c). Complementing *lrhA* restored transcription of *cse1* in BW25113 Δ*hns* Δ*leuO* mutants (Fig. S7), confirming that LrhA is able to activate P_{cas} (Fig. 2e). In contrast to moderate activation of the *cas* operon by LrhA, LeuO exhibited a stronger stimulation effect on P_{cas}. In both BW25113 Δ*hns* and Δ*hns* Δ*lrhA* mutants, deleting *leuO* decreased transcription of *cse1* by more than 60% (Fig. 2c).

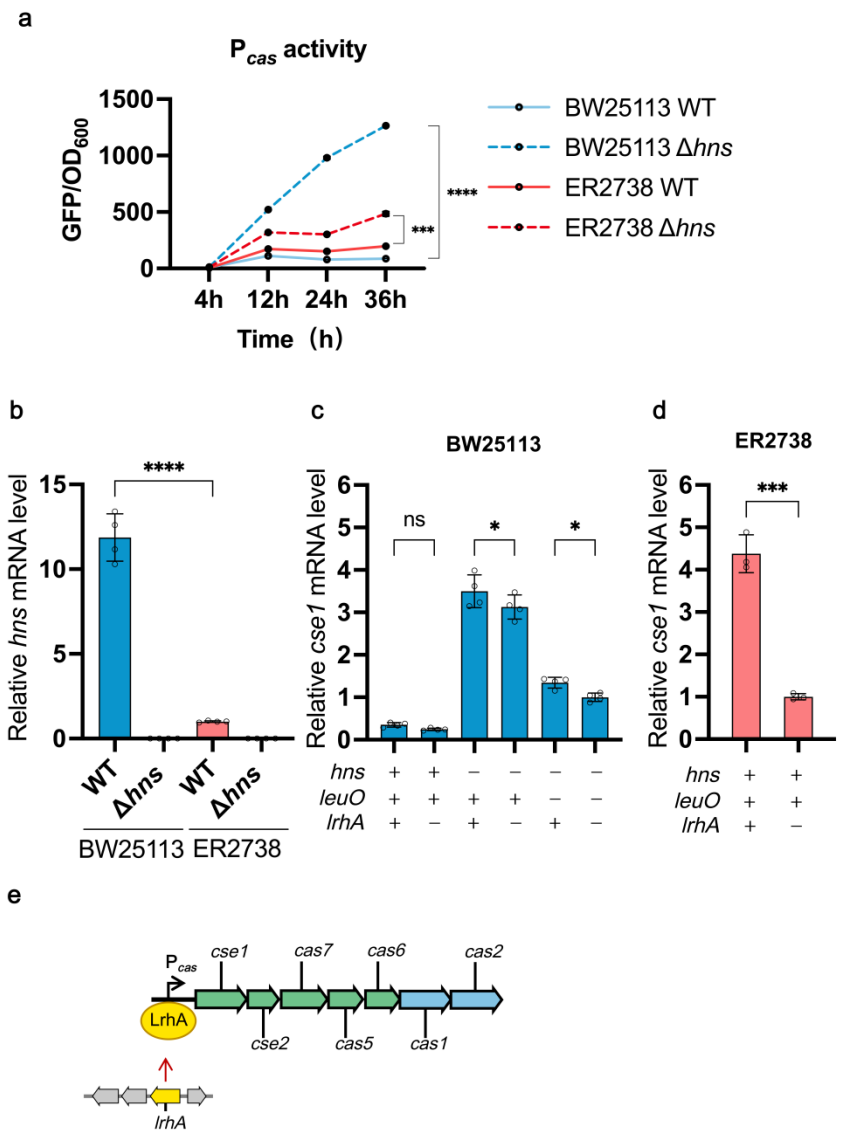

Figure 2. LrhA activates transcription of the *cas* operon by binding to P_{cas}. (**a**) The P_{cas} activity of BW25113 WT (blue solid line), BW25113 Δ*hns* (EC71) (blue dashed line), ER2738 WT (red solid line) and ER2738 Δ*hns* (EC74) (red dashed line) cells grown at 37 ℃, which was evaluated by GFP/OD_{600}. Statistical significance was assessed using a two-way ANOVA ($n = 3$). ****, $P < 0.0001$; ***, $P < 0.001$. (**b**) qPCR analysis of *hns* in BW25113 WT, BW25113 Δ*hns* (EC71), ER2738 WT and ER2738 Δ*hns* (EC94) cells grown at 37 ℃ for 36 h, with the relative expression level of ER2738 Δ*hns* as 1 arbitrary unit. Statistical significance was assessed using a one-way ANOVA. Bars are the means and error bars ± SD. ****, $P < 0.0001$. Individual biological replicates are shown ($n = 4$). (**c**) Effects of genomic *lrhA* on the P_{cas} activity (indicated by *cse1*) assessed by qPCR assay. P_{cas} activities were compared in BW25113 WT, Δ*lrhA* (EC75), Δ*hns* (EC71), Δ*hns* Δ*lrhA* (EC76) strain, Δ*hns* Δ*leuO* (EC73), and BW25113 Δ*hns* Δ*leuO* Δ*lrhA* (EC77) grown in LB medium at 37 ℃ for 36 h, with the relative expression level of BW25113 Δ*hns* Δ*leuO* Δ*lrhA* as 1 arbitrary unit. Statistical significance was assessed using a one-way ANOVA. *, $P < 0.05$. Individual biological replicates are shown ($n = 4$). (**d**) qPCR analysis of *cse1* in ER2738 WT and ER2738 Δ*lrhA* (EC87) cells grown at 37 ℃, with the relative expression level of ER2738 Δ*lrhA* as 1 arbitrary unit. Statistical significance was assessed using a two-tailed Student' s t-test. ***, $P < 0.001$. Individual biological replicates are shown ($n = 3$). (**e**) Schematic depiction of the regulation of P_{cas} by LrhA.

223 The LrhA-binding site was reported to partially overlap with a LeuO-binding site on the
224 promoter of *leuO*[70]. Previous work has identified two LeuO binding sites (LBS I and LBS
225 II) within P_{cas} [60, 61] (Fig. S1). The observation that the presence of LeuO interfered with the
226 regulation of P_{cas} by LrhA prompted us to consider whether LrhA and LeuO compete for
227 the same binding sites on P_{cas}. To check this, DNA probes lacking LBS I and/or LBS II
228 were generated (named 'P_{cas} del LBS I', 'P_{cas} del LBS II', and 'P_{cas} short probe') and
229 EMSA was employed to determine the effect of LBS I and LBS II on the efficiency of
230 LrhA binding to P_{cas}. As shown in Fig. 3a, 700 nM of His-LrhA was sufficient to retard the
231 mobility of the full-length P_{cas} probe (P_{cas} FL). However, deleting LBS I resulted in the
232 abolishment of LrhA binding with P_{cas}, even the concentration of LrhA reached 1400 nM,
233 while deleting LBS II only partially impaired LrhA binding with P_{cas}. (Fig. 3a). These
234 observations support that LrhA binds to both LBS I and LBS II.
235 To know whether LBS I and LBS II were essential to activate P_{cas} by LrhA and LeuO *in*
236 *vivo*, we generated P_{cas} containing disrupted LBS I and/or LBS II (Fig. 3b), and compared
237 *in vivo* activities of disrupted P_{cas} with that of P_{cas} FL in response to expression of LrhA
238 and LeuO. Over-expressing LrhA and LeuO increased the transcriptional activity of P_{cas}
239 FL by more than 3- and 8-fold, respectively (Fig. 3b). In contrast, the activity of P_{cas} del
240 LBS I in the BW25113 Δ*hns* Δ*leuO* mutant expressing LrhA or LeuO was decreased to the
241 background level or 3.88-fold higher than the background level, respectively (Fig. 3b). This
242 observation indicates that LBS I is indispensable for activation of P_{cas} by LrhA, and
243 essential for full stimulation of P_{cas} by LeuO. Interestingly, the activity of P_{cas} del LBS II
244 was also remarkably reduced in the BW25113 Δ*hns* Δ*leuO* mutant expressing either LrhA
245 or LeuO (Fig. 3b), revealing that LBS II is required for activation of P_{cas} by both LrhA and
246 LeuO. As expected, when both LBS I and LBS II were deleted, the expression of LrhA or
247 LeuO no longer stimulated the expression of the impaired P_{cas} (Fig. 3b). Taken together,
248 these data clearly show that both LBS I and LBS II are essential for activation of P_{cas} by
249 LrhA and LeuO *in vivo*.

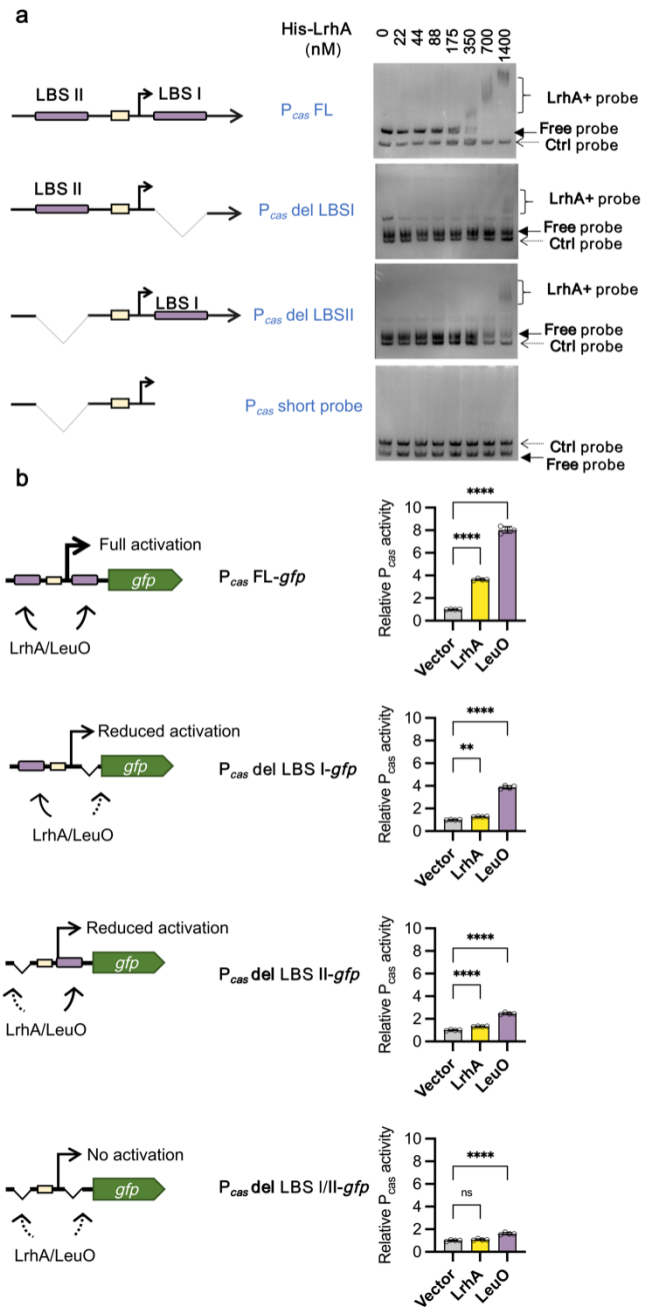

Figure 3. Identification of LrhA binding sites on the promoter of the *cas* operon. (**a**) (**left**) Schematic illustration of the P_{cas} region for truncation analysis. LBS I and LBS II indicate two DNA-binding sites of LeuO located upstream and downstream of the transcriptional start site (TSS, black arrow) on P_{cas} (purple bars). HBS indicates the DNA-binding site of the H-NS (yellow bar). (**right**) electrophoretic mobility shift (EMSA) assays of full-length or truncated P_{cas} DNA fragments by LrhA. The P_{cas} probes including full-length P_{cas} (P_{cas} FL), P_{cas} with LBS I deleted (P_{cas} del LBS I), P_{cas} with LBS II deleted (P_{cas} del LBS II) and P_{cas} with both LBS I and LBS II deleted (P_{cas} short probe) were generated. 1 nM P_{cas} probes were separately incubated with a serial concentration of purified His-LrhA before EMSA assays with 5% native polyacrylamide gels (solid arrow for free P_{cas} probes, and braces for LrhA+probe complex). A 175 bp probe of *lacZα* fragment was used as the control (Ctrl probe, dashed arrow). (**b**) (**left**) Schematic illustration of DNA binding sites required for activating P_{cas} by LrhA and LeuO. Transcriptional activities of full-length P_{cas}, P_{cas} del LBS I, P_{cas} del LBS II and P_{cas} del LBS I/II were compared by using the P_{cas}-*gfp* reporter. (**right**) Effects of

disruption of LBS I and LBS II on activation of P_{cas} by LrhA. The P_{cas} activity was evaluated by GFP/OD_{600}, with the relative expression level of BW25113 Δ*hns* Δ*leuO* carrying the empty vector as 1 arbitrary unit. Bars are the means and error bars ± SD. Individual biological replicates are shown (n = 4). Statistical significance was determined using one-way ANOVA with Dunnett's multiple comparisons test. ****, $P < 0.0001$; **, $P < 0.01$.

LrhA activates CRISPR interference against M13 phage infection

Having established LrhA as a regulator of P_{cas}, we sought to test whether it could play a role in regulating CRISPR interference against bacteriophage in the wild-type *E. coli* ER2738, which contains an F-factor encoding pili that are required for M13 phage adsorption [71]. A spacer (g8 spacer) matching the gene 8 of M13 phage was integrated into the CRISPR I array of the wild-type ER2738 strain (WT-g8), which was expected to confer resistance to M13 phage infection (Fig. 4a). The ER2738 Δ*lrhA* mutant showed swarm rings with increased diameter compared with ER2738 WT (Fig. S6c). Inactivation of *lrhA* in ER2738-g8 (Δ*lrhA*-g8) reduced the efficiency of plaquing (EOP) by ~10^6-fold, while complementing *lrhA* in the *ΔlrhA* mutant (*lrhA*^{c}-g8) fully restored its resistance to M13 phage (Fig. 4b), revealing that LrhA expressed from the genome strongly activates the CRISPR-Cas immunity against infection of the phage. Inactivation of *cas3* abolished the CRISPR immunity in WT-g8 (Fig. S8). Together, these results demonstrate that LrhA plays a crucial role in promoting the CRISPR interference against phage infection in a wild-type *E. coli* strain (Fig. 4c).

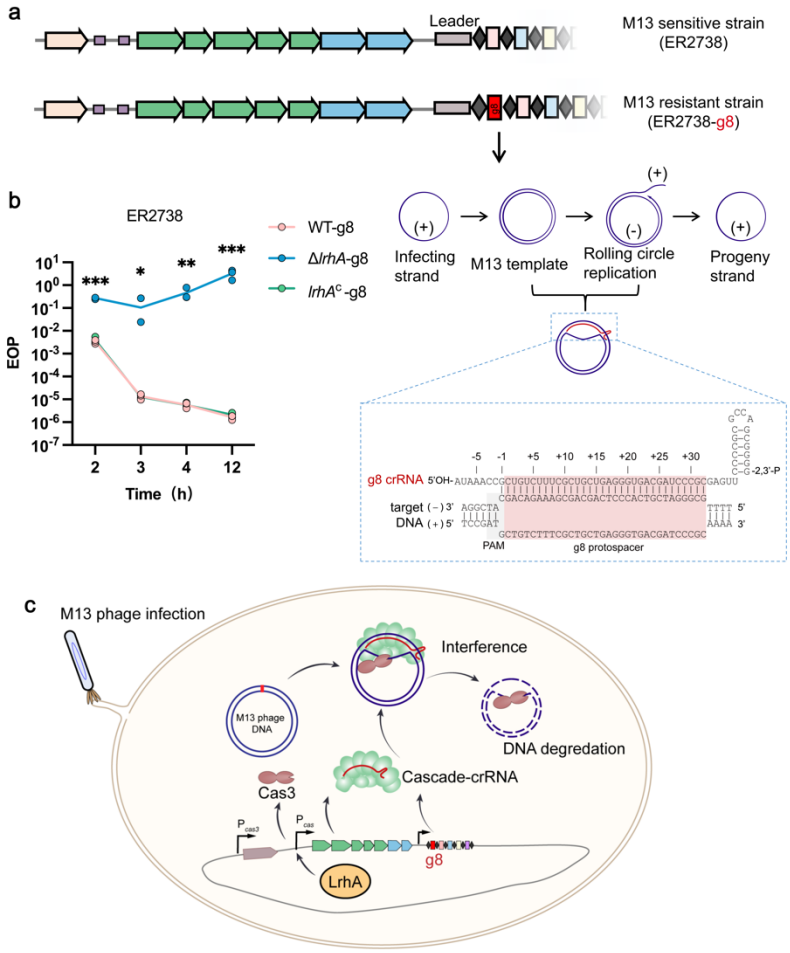

Figure 4. LrhA activates CRISPR-Cas immunity against M13 phage. (**a**) Schematic illustration of the engineered CRISPR cassette carrying a g8 spacer in the genomic CRISPR I locus. In M13 targeting cells, CRISPR I contains an additional g8 spacer (red rectangle), conferring cells with resistance to M13 phage infection. During infection, phage DNA enters the cell as a circular (+) single-stranded (ss) DNA, followed by the formation of double-stranded (ds) phage genome DNA (template), which is replicated in a rolling circle form to generate progeny (+) strand that is packaged in mature phage. M13 phage DNA in the dsDNA form (i.e., template and rolling circle replication) can be recognized by g8 crRNA-guided Cascade complex. (**b**) Quantification of the efficiency of plating (EOP) at 2-12 h after infection with M13 phage. Efficiency of plaquing (EOP) was calculated as a ratio of phage titers observed on cells with g8 spacer (WT-g8, EC89; Δ*lrhA*-g8, EC90 and *lrhAc*-g8, EC91) to that on cells without g8 spacer (non-targeting cells, WT, ER2738; Δ*lrhA*, EC87 and *lrhA*^{c}, EC88). Individual biological replicates are shown (n = 3). Statistical significance between WT-g8 and Δ*lrhA*-g8 at 2-12h was determined using multiple t-tests. *, P < 0.05; **, P < 0.01; ***, P < 0.001 (**c**) Schematic illustration of regulation of the CRISPR-Cas system against M13 phage infection by LrhA.

LrhA promotes clearance of the CRISPR-targeted plasmid

We examined the role of LrhA on transferring and transferred CRISPR-targeted plasmids. Although deletion of *lrhA* showed no effect on CRISPR immunity against pTc during conjugation (Fig. S9a-c), we observed that LrhA promoted CRISPR immunity against the transferred CRISPR-targeted plasmid in *E. coli* BW25113 lacking *hns* and/or *leuO*. The CRISPR immunity against transferred plasmid was assessed by evaluating the clearance rate of CRISPR-targeted plasmid in *lrhA*$^+$ and *lrhA*$^-$ strains. The relative CRISPR immunity in the *lrhA*$^+$ strain was ~3.5-fold of that in the *lrhA*$^-$strain with deletion of *hns* (Fig. 5a-b) and ~9.8-fold of that in the *lrhA*$^-$ strain with further deletion of *leuO* (Fig. 5b), demonstrating that LrhA activates type I-E CRISPR-Cas system for clearing the CRISPR-targeted plasmid independent upon H-NS and LeuO. Given that deleting *leuO* led LrhA to exhibit a stronger effect on promoting clearance of CRISPR-targeted plasmid, promotion of the CRISPR immunity by LrhA could be partially masked by LeuO.

Promoting primed adaptation by LrhA accelerates clearance of the CRISPR-targeted plasmid

We observed an apparent effect of LrhA on CRISPR immunity against transferred plasmid during long-term growth but not transferring plasmid during conjugation. Given that weak interference often allows DNA to persist longer and promotes acquisition of new spacers that allows bacteria to mount more efficient CRISPR interference [32, 34, 72], we hypothesized that intermediate activation of the *cas* operon by LrhA might promote clearance of pT through better coordinating interference and primed adaptation. To test this hypothesis, we monitored CRISPR array expansion in response to pT and pNT in *lrhA*$^+$ and *lrhA*$^-$ strains (Fig. 5d). Compared with that in the *lrhA*$^+$ strain, fewer expansion events were observed in the *lrhA*$^-$ mutant carrying pT after 36 h of incubation at 37 °C, showing that LrhA is required for efficient adaptation (Fig.5e, Fig. S10). Complementing *lrhA* on the genome of the *lrhA*$^-$ mutant (*lrhA*^{c}) restored adaptation (Fig. 5f). In contrast, CRISPR array expansion was not observed in the *lrhA*$^+$ and *lrhA*$^-$strains carrying pNT (Fig. 5e). Sequencing analysis of the expansion bands from *lrhA*$^+$ strains carrying pT revealed that all newly formed spacers (20/20) were derived from the CRISPR targeted plasmid (Fig. 5g), with a strong preference for an AAG PAM (16/20) during adaptation, and a pronounced bias in the DNA strand (15/20) matching the orientation of the CRISPR-targeting units (CR1) (Table S3), in agreement with typical traits of primed CRISPR adaptation[32, 34]. Compared with other

regions on the CRISPR-targeted plasmid, more protospacers were mapped to encoding genes (i.e., *bla* and *dsRED*) and the replication origin (Fig. 5g).

To confirm that LrhA promoted clearance of pT through reinforcing the interplay between CRISPR-Cas interference and primed adaptation, we deleted both *cas1* and *cas2* (Δ*cas1-2*) in *lrhA*$^{+}$, *lrhA*$^{-}$ and *lrhA*^{c} strains, and examined the CRISPR interference in these strains through the plasmid loss assay. Deletion of *cas1-cas2* abolished the CRISPR array expansion (Fig. 5f), and reduced the effect of LrhA on CRISPR immunity against plasmid (Fig. 5c, Fig S11), revealing that LrhA activates CRISPR immunity through promoting the positive feedback of interference and adaptation processes (Fig. 5h). Loss of CRISPR expansion from Δ*cas1-2* cells was restored by genomic complementation of *cas1-cas2* (*cas1-2*^{c}) (Fig. 5f), consistent with critical role of *cas1-cas2* in adaption. Activation of CRISPR interference by LrhA was regained by complementation of *cas1-cas2* (Fig. S11), confirming that Cas1-Cas2 was essential to LrhA-regulated adaptation-mediated interference.

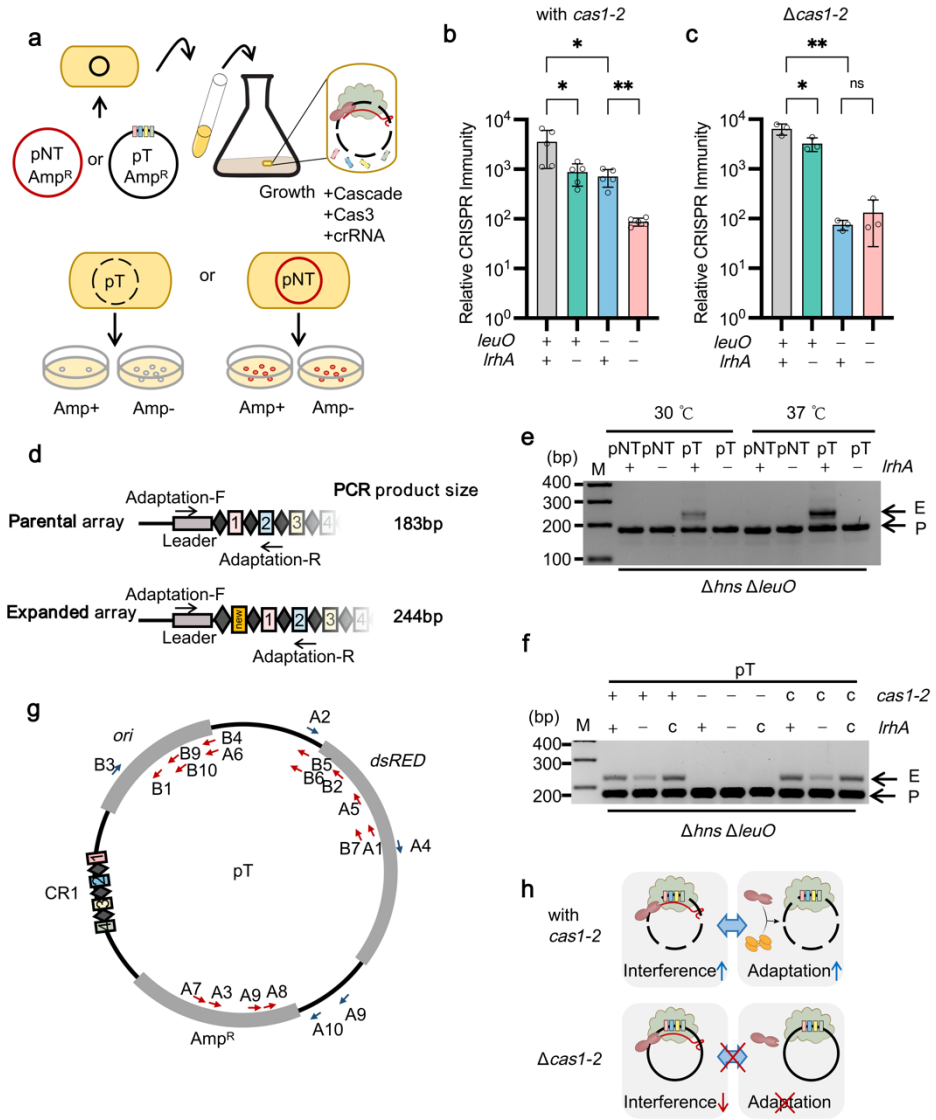

Figure 5. LrhA activates both CRISPR-Cas interference and adaptation. (**a**) Schematic illustration for evaluating the CRISPR-Cas interference activity by plasmid loss assay. (**b** and **c**) Relative CRISPR immunity assessed by plasmid loss assay in *E. coli* strains BW25113 Δ*hns* (EC71), Δ*hns* Δ*lrhA* (EC76), Δ*hns* Δ*leuO* (*lrhA*$^+$, EC73) and Δ*hns* Δ*leuO* Δ*lrhA* (*lrhA*$^-$, EC77) grown in antibiotic-free LB medium for 36 h. Statistical significance was assessed using a two-tailed Student' s t-test. Bars are the means and error bars ± SD. Individual biological replicates are shown (n = 5 for *b* and n = 3 for c). *, $P < 0.05$; **, $P < 0.01$. (**d**) Schematics of the spacer acquisition assay in (**e** and **f**). During the adaptation process, a new spacer (a yellow rectangle) can be inserted into the leader end of the CRISPR array. PCR was performed to amplify the leader-spacer region using the primers matching the leader and the second spacer, which were indicated as flagged arrows. (**e**) Spacer-acquisition assay by PCR amplification of BW25113 Δ*hns*Δ*leuO* (*lrhA*$^+$, EC73), BW25113 Δ*hns* Δ*leuO* Δ*lrhA* (*lrhA*$^-$, EC77) cells carrying pT or pNT plasmids, which were grown at 37 ℃ or 30 ℃ for 36 h. PCR products were electrophoresed on a 2% agarose gel and imaged. Parental (P) and expanded bands (E) are indicated on the right while DNA marker (M) positions are displayed on the left. Gels are representative of two experiments yielding similar results. (**f**) spacer-acquisition assay of *lrhA*$^+$, *lrhA*$^-$ and *lrhA*^{c} with *cas1-cas2* deletion (Δ*cas1-2,* EC81, EC82, EC83) or its complementation (*cas1-2* ^{c}, EC84, EC85, EC86). (**g**) Mapping of newly formed spacers on pT plasmid DNA. The DNA of the expanded array was sequenced by ligating purified PCR products into T vectors. The position and orientation of the sequenced spacers are marked on the pT plasmid map (blue arrows pointing clockwise and red arrows pointing counterclockwise). Protospacers are numbered according to the strain from which the spacers were sequenced, as listed in Table S3. CR1 indicates 4 spacers targeted by the type I-E CRISPR-Cas system of *E. coli*. (**h**) Schematic illustration of the relationship between CRISPR interference and adaptation regulated by LrhA. In the presence of *cas1-2*, LrhA promotes the positive feedback circuit between CRISPR interference and adaptation (upper panel). In the absence of *cas1-2*, LrhA shows a weak effect on interference (lower panel).

DISCUSSION

In this study, we have addressed the important question of how the CRISPR-Cas system is regulated through coordinating interference and adaptation. By combining DNA pull-down and mass spectrometry, we identified a novel regulator, LrhA, that enhances immunity against phage infections by directly blocking the entry of phage DNA and facilitates a reciprocal interplay between interference and adaptation, thereby providing protection against horizontally transferred plasmids in *E. coli*. Our study not only provides new insights into how bacteria control the adaptive immunity against exogenous DNA under different scenarios, adding a new layer of regulatory complexity in bacterial defense, but also introduces a functional approach to screen any transcriptional regulators that directly bind to promoters in bacteria.

Early reports suggested that primed adaptation was triggered by suboptimal Cascade-protospacer interactions that could lead to weak interference[32, 58, 73], whereas others indicated that optimal Cascade-protospacer interactions also led to both interference and primed adaptation, which was fueled by interference[35, 53, 72, 74]. Evidence remains lacking for intracellular regulation of CRISPR immunity through coordination of interference and adaptation. In this study, we found that LrhA moderately stimulated transcription of *cas* genes but strongly promoted the clearance of CRISPR-targeted plasmid. Adaptation occurred more frequently in the *lrhA*$^+$ *E. coli* strains harboring the CRISPR-targeted plasmid (Fig. 5, and Fig. S10), revealing that LrhA can promote interference-driven spacer acquisition. Given that inactivation of *cas1* and *cas2* remarkably reduced LrhA-stimulated CRISPR immunity (Fig. 5c), we propose that moderate activation of transcription of *cas*

genes by LrhA enables the positive feedback circuit between CRISPR interference and adaptation: cleavage of the CRISPR-targeted plasmid produces more short DNA fragments for accelerating primed adaptation, which in turn enhances clearance of the CRISPR-targeted plasmid (Fig. S12). In contrast, strong activation of transcription of *cas* genes by LeuO was unlikely to trigger the positive feedback circuit, and exhibited weaker effect on clearance of the CRISPR-targeted plasmid. Analysis of the acquired spacers revealed an unequal distribution (Fig. 5g), suggesting that certain sequences could be preferentially integrated as new spacers.

The transcriptional regulators of type I-E CRISPR-Cas system have not been screened thoroughly. In a previous study of identification of the potential host factors involved in adaptation, Yoganand *et al* employed the CRISPR/dCas9 mediated immunoprecipitation (IP) to identify host factors that bound the CRISPR leader region[75]. Compared to the reported CRISPR/dCas9-mediated IP screening strategy, the pull-down assay employed in this study is significantly simpler and facilitates the identification of a larger number of potential proteins, owing to the ease of obtaining sufficient amounts of biotin-labeled probes, albeit at the expense of increased false positive detection. Nevertheless, subsequent screening with a fluorescence reporter helps to the presence of unwanted proteins. By using the DNA pull-down assay with a DNA probe containing P_{cas} as the bait, we screened out a number of host factors that associated with P_{cas} from the cell lysate. Particularly, both our *in vivo* and *in vitro* data reveal that the pleiotropic LTTRs LrhA activate the *cas* operon by binding to the LeuO binding sites in P_{cas}. LTTR family proteins seem to extensively regulate diverse types of CRISPR-Cas systems in different bacteria. LrhA (named PigU in *Serratia*) was reported to suppress the type III and type I-F but not the type I-E CRISRP-Cas system[76], indicating that this regulator plays differential roles in different bacteria. In *Salmonella enterica*, transcription of the CRISPR-Cas system was by two LTTRs with opposing functions (i.e., LeuO and LRP) [77]. LeuO is normally considered as an antagonist of H-NS, and activates gene transcription by relieving transcriptional suppression by H-NS, we found that both LrhA and LeuO promoted the activity of P_{cas} in the Δ*hns* Δ*leuO* mutants (Fig. 1e, Fig. 2c), indicating that they both regulate the *cas* operon independent of H-NS.

Although both LrhA and LeuO bind P_{cas}, their impacts on regulation of the type I-E CRISPR-Cas system and other physiological functions are context-dependent. LrhA strongly stimulated the CRISPR-Cas activity against M13 phage in the wild-type *E. coli* ER2738 (Fig. 4b), demonstrating that LrhA is capable of playing a dominant role in regulating CRISPR-Cas activity in *E. coli* upon phage infection. Roles of LeuO and LrhA are also different in regulating the CRISPR-Cas activity for clearing horizontally transferred plasmid. Although LeuO stimulated stronger transcription of *cas* genes, LrhA stimulated higher adaptive immunity in clearing CRISPR-targeted plasmid through better-coordinating interference and adaptation. The two regulators show different binding site dependencies at P_{cas}. Apart from regulating the CRISPR-Cas system, LrhA and LeuO showed remarkable differences in controlling other physiological functions, such as the flagellar *flhDC* operon, which can be inhibited by LrhA, but not LeuO (Fig. S6). Moreover, LeuO activated transcription of the *cas* operon through direct interacting with the α subunit of the RNA polymerase (RpoA) on P_{cas}, but the regulation of P_{cas} by LrhA seemed independent of RpoA (unpublished data). Phylogenetic analysis revealed divergent evolution of LrhA and LeuO, which could belong to distinct subfamilies and separately

evolve in bacteria (Fig. S13 and S14).The expression of LeuO can be activated by the heterodimer BglJ-RcsB[78], Cyanase regulator CynR[70], and antibiotic responses regulator YdcI[70], while the expression of LrhA is stimulated by acid resistance-related gene *hdeD* [79]. Hence, the regulation of the type I-E CRISPR-Cas system by LrhA and LeuO could have been developed in response to different environmental cues.

MATERIALS AND METHODS

Bacterial strains, plasmids, primers, growth conditions, and media

Bacterial strains, plasmids, and primers used in this study are listed in *Supplementary information* Table S4, Table S5 and Table S6. *E. coli* gene-deletion mutants were constructed by using a λ-RED recombination system expressed by the temperature-sensitive plasmid pKD46 [80]. Corresponding mutants were examined through PCR. Recombinant plasmids expressing LrhA and other 10 TFs were constructed with a Transfer PCR method [81]. Plasmids were isolated and purified with a plasmid isolation kit according to the manufacturer's protocol (Axygen Biotech Co., Ltd.). *E. coli* cultures were grown at 37 ℃ in LB broth medium containing 1% (wt/vol) tryptone, 0.5% (wt/vol) yeast extract, and 1% (wt/vol) NaCl or on LB agar plates containing 1.5% (wt/vol) agar. When required, media were supplemented with ampicillin (100 μg mL^{-1}), kanamycin (50 μg mL^{-1}), or chloramphenicol (25 μg mL^{-1}). Arabinose was added for inducing gene expression in liquid cultures where indicated. Cell growth was measured in a spectrophotometer (MD SpectraMax iD5 or Biotek Synergy 2). All experiments were repeated independently at least three times unless otherwise indicated.

Pull-down assay

P_{cas}-binding proteins were pulled-down with the streptavidin beads (Invitrogen Dynabeads™ M-270, 65305) according to the manufacturer's protocol. (see "Pull-down assay" in *Supplementary information* Supplementary Methods).

Mass spectrometry analysis

Mass spectrometry and analysis of the data were conducted by Micrometer Biotech Company. (see "Mass spectrometry analysis" in *Supplementary information* Supplementary Methods).

Quantification of gene transcription

For quantifying P_{cas} with reporter assay, plasmid pGLO-P_{cas}-*gfp* was used for monitoring the transcription of the *cas* operon, by measuring the intensity of GFP fluorescence and cell optical density (OD_{600}) on a microplate reader (MD, SpectraMax iD5), with a method that has previously been described[64]. When evaluating the GFP/OD_{600} level or the interference/adaptation effect, cells were grown in M9 minimal medium containing 61 mM $K_2HPO_4 \cdot 3H_2O$, 38.21 mM KH_2PO_4, 2.5 mM $MgSO_4$, 15.14 mM $(NH_4)_2SO_4$, 0.1% (wt/vol) tryptone, supplemented with 1% (wt/vol) glucose as the carbon source.

For the quantitative real-time PCR (qPCR) assay, bacteria were harvested from 0.4-1mL culture by centrifugation. Total RNA was extracted by using an RNA Extraction Kit (AG21017, Accurate Biotechnology Co., Ltd). Removal of the genomic DNA and reverse transcription were performed by using Evo M-MLV RT Mix Kit (with gDNA clean reaction mix) (AG11728) according to the manufacturer's

instructions. SYBR Green Premix Pro Taq HS qPCR Kit (AG11701) was used for qPCR, and the cycle thresholds were determined using a BioRad CFX96 Real-Time System. *rpoD* was used as the internal control. The primers for *cse1* and *rpoD* are listed in Table S6.

Purification of LrhA Protein

The LrhA protein was purified by Ni-NTA Resin (ThermoFisher, 88222), according to the manufacturer's protocol. (see "Purification of LrhA Protein" in *Supplementary information* Supplementary Methods).

Electrophoretic mobility shift assay (EMSA)

EMSA was performed by using the LightShift Chemiluminescent EMSA kit (ThermoFisher, 20148) according to the manual guide. For more details, see "Electrophoretic mobility shift assay" in *Supplementary information* Supplementary Methods.

Plasmid loss assay

The *E. coli* strains harboring the CRISPR-targeted plasmid pT (p*dsRED*-CR1) or the CRISPR-non-targeted plasmid pNT (p*dsRED*) were grown overnight in LB culture supplemented with ampicillin (100 μg mL^{-1}). The overnight grown culture was washed and inoculated at a ratio of 2% into antibiotic-free LB medium, followed by incubation at 37 ℃ with shaking. At intervals, the culture was serially diluted and spread on the LB plate supplemented with or without ampicillin (100 μg mL^{-1}). The number of cells maintained the plasmid was evaluated by comparing colonies on the LB plate supplemented with or without ampicillin. The relative CRISPR immunity was defined as the proportion of cells containing the pNT plasmid relative to that containing the pT plasmid.

Spacer acquisition assay

Newly acquired spacers were detected by PCR using primers pair Adaptation-F and Adaptation-R. (see "Spacer acquisition assay" in *Supplementary information* Supplementary Methods).

M13 phage sensitivity assay.

E. coli ER2738 strains with or without chromosomal g8 spacers were grown in LB medium supplemented with M13 phage with a titer of 10^6 plaque-forming units (PFU) per mL at 37 ℃. PFU of M13 phages from these bacterial cultures were counted at the indicated time points through a documented method [32, 48]. Briefly, the supernatants were diluted tenfold, then mixed with 100 μL ER2738 (OD_{600} ~ 0.5). The mixture was spread in 1 mL 0.75 % LB top agar and overlaid on LB plates containing 0.2 mM IPTG (isopropyl-β-D-thiogalactoside) and 40 μg mL^{-1} X-Gal (5-bromo-4-chloro-3-indolyl-b-Dgalactopyranoside) for visualization of M13 phage which carries the *lacZα* gene. After incubation at 37 ℃ overnight, the plaque-forming units (PFU) on plates were counted. Efficiency of plaquing (EOP) was calculated as a ratio of phage titers observed on cells with g8 spacer to that on cells without g8 spacer (non-targeting cells).

ACKNOWLEDGMENTS

We thank Prof. Shishen Du at Wuhan University and Dr. Yanmei Zhang at Hangzhou Medical College for scientific advice on this manuscript. We also thank Prof. Zhiyong Sun at Zhejiang University of Technology, Prof. Pengjun Zhang at

Hangzhou Normal University, Dr. Minjia Shen at Université Paris-Saclay, Ms. Xia Yao at Zhejiang University of Technology, and all members of the Sun laboratory for critically reading the manuscript and helpful discussions. We also would like to express our sincere gratitude to the editor and three anonymous reviewers for their valuable comments, which have greatly improved the quality of the manuscript.

Funding

This work was supported by the National Natural Science Foundation of China (grants 32170083 and 31670084), the Key Research and Development Program of Zhejiang Province (grant 2020C02031).

REFERENCES

1. Duan B, Ding P, Navarre WW, Liu J, Xia B. Xenogeneic silencing and bacterial genome evolution: mechanisms for DNA recognition imply multifaceted roles of xenogeneic silencer. *Mol Biol Evol* **38**, 4135-4148 (2021).

2. Horvath P, Barrangou R. CRISPR/Cas, the immune system of bacteria and archaea. *Science* **327**, 167-170 (2010).

3. Liu X*, et al.* Xenogeneic silencing relies on temperature-dependent phosphorylation of the host H-NS protein in *Shewanella*. *Nucleic Acids Res* **49**, 3427-3440 (2021).

4. Shi WT, Zhang B, Li ML, Liu KH, Jiao J, Tian CF. The convergent xenogeneic silencer MucR predisposes alpha-proteobacteria to integrate AT-rich symbiosis genes. *Nucleic Acids Res* **50**, 8580-8598 (2022).

5. Makarova KS*, et al.* Evolutionary classification of CRISPR-Cas systems: a burst of class 2 and derived variants. *Nat Rev Microbiol* **18**, 67-83 (2020).

6. Mohanraju P, Makarova KS, Zetsche B, Zhang F, Koonin EV, van der Oost J. Diverse evolutionary roots and mechanistic variations of the CRISPR-Cas systems. *Science* **353**, aad5147 (2016).

7. Hille F, Richter H, Wong SP, Bratovič M, Ressel S, Charpentier E. The biology of CRISPR-Cas: backward and forward. *Cell* **172**, 1239-1259 (2018).

8. Koonin EV, Makarova KS, Zhang F. Diversity, classification and evolution of CRISPR-Cas systems. *Curr Opin Microbiol* **37**, 67-78 (2017).

9. Garneau JE*, et al.* The CRISPR/Cas bacterial immune system cleaves bacteriophage and plasmid DNA. *Nature* **468**, 67-71 (2010).

10. Marraffini LA, Sontheimer EJ. CRISPR interference limits horizontal gene transfer in S*taphylococci* by targeting DNA. *Science* **322**, 1843-1845 (2008).

11. Barrangou R*, et al.* CRISPR provides acquired resistance against viruses in prokaryotes. *Science* **315**, 1709-1712 (2007).

12. Horvath P*, et al.* Diversity, activity, and evolution of CRISPR loci in *Streptococcus thermophilus*. *J Bacteriol* **190**, 1401-1412 (2008).

13. Deveau H*, et al.* Phage response to CRISPR-encoded resistance in *Streptococcus thermophilus*. *J Bacteriol* **190**, 1390-1400 (2008).

14. Amitai G, Sorek R. CRISPR-Cas adaptation: insights into the mechanism of action. *Nat Rev Microbiol* **14**, 67-76 (2016).

15. Lee H, Sashital DG. Creating memories: molecular mechanisms of CRISPR adaptation. *Trends Biochem Sci* **47**, 464-476 (2022).

16. Levy A*, et al.* CRISPR adaptation biases explain preference for acquisition of foreign DNA. *Nature* **520**, 505-510 (2015).

17. Sternberg SH, Richter H, Charpentier E, Qimron U. Adaptation in CRISPR-Cas systems. *Mol Cell* **61**, 797-808 (2016).

18. Patterson AG, Yevstigneyeva MS, Fineran PC. Regulation of CRISPR-Cas adaptive immune systems. *Curr Opin Microbiol* **37**, 1-7 (2017).

19. Shivram H, Cress BF, Knott GJ, Doudna JA. Controlling and enhancing CRISPR systems. *Nat Chem Biol* **17**, 10-19 (2021).

20. Pacesa M, Loeff L, Querques I, Muckenfuss LM, Sawicka M, Jinek M. R-loop formation and conformational activation mechanisms of Cas9. *Nature* **609**, 191-196 (2022).

21. Xiao Y*, et al.* Structure basis for directional R-loop formation and substrate handover mechanisms in type I CRISPR-Cas system. *Cell* **170**, 48-60 (2017).

22. Selle K, Barrangou R. Harnessing CRISPR-Cas systems for bacterial genome editing. *Trends Microbiol* **23**, 225-232 (2015).

23. Baumann K. Genome editing: CRISPR-Cas becoming more human. *Nat Rev Mol Cell Biol* **18**, 591 (2017).

24. Stella S, Alcón P, Montoya G. Class 2 CRISPR-Cas RNA-guided endonucleases: Swiss Army knives of genome editing. *Nat Struct Mol Biol* **24**, 882-892 (2017).

25. Wang JY, Pausch P, Doudna JA. Structural biology of CRISPR-Cas immunity and genome editing enzymes. *Nat Rev Microbiol* **20**, 641-656 (2022).

26. Bikard D EC, Jiang W, et al. Exploiting CRISPR-Cas nucleases to produce sequence-specific antimicrobials. *Nat Biotechnol* **32**, 1146-1150 (2014).

27. Citorik RJ MM, Lu TK. Sequence-specific antimicrobials using efficiently delivered RNA-guided nucleases. *Nat Biotechnol* **32**, 1141-1145 (2014).

28. Kiga K TX, Ibarra-Chavez R, et al. Development of CRISPR-Cas13a-based antimicrobials capable of sequence-specific killing of target bacteria. *Nat Commun* **11**, 2934 (2020).

29. Selle K FJ, Tuson H, et al. *In vivo* targeting of *Clostridioides difficile* using phage-delivered CRISPR-Cas3 antimicrobials. *mBio* **11**, e00019-00020 (2020).

30. Neil K*, et al.* High-efficiency delivery of CRISPR-Cas9 by engineered probiotics enables precise microbiome editing. *Mol Syst Biol* **17**, e10335 (2021).

31. Fang M*, et al.* Engineering probiotic *Escherichia coli* Nissle 1917 to block transfer of multiple antibiotic resistance genes by exploiting a type I CRISPR-Cas system. *bioRxiv*, 2024.2004.2001.587504 (2024).

32. Datsenko KA, Pougach K, Tikhonov A, Wanner BL, Severinov K, Semenova E. Molecular memory of prior infections activates the CRISPR/Cas adaptive bacterial immunity system. *Nat Commun* **3**, 945 (2012).

33. Fineran PC, Charpentier E. Memory of viral infections by CRISPR-Cas adaptive immune systems: acquisition of new information. *Virology* **434**, 202-209 (2012).

34. Swarts DC, Mosterd C, van Passel MW, Brouns SJ. CRISPR interference directs strand specific spacer acquisition. *PLoS ONE* **7**, e35888 (2012).

35. Semenova E*, et al.* Highly efficient primed spacer acquisition from targets destroyed by the *Escherichia coli* type I-E CRISPR-Cas interfering complex. *Proc Natl Acad Sci USA* **113**, 7626-7631 (2016).

36. Vale PF, Lafforgue G, Gatchitch F, Gardan R, Moineau S, Gandon S. Costs of CRISPR-Cas-mediated resistance in *Streptococcus thermophilus*. *Proc Biol Sci* **282**, 20151270 (2015).

37. Jiang W, Maniv I, Arain F, Wang Y, Levin BR, Marraffini LA. Dealing with the evolutionary downside of CRISPR immunity: bacteria and beneficial plasmids. *PLoS Genet* **9**, e1003844 (2013).

38. Stern A, Keren L, Wurtzel O, Amitai G, Sorek R. Self-targeting by CRISPR: gene regulation or autoimmunity? *Trends Genet* **26**, 335-340 (2010).

39. Vercoe RB*, et al.* Cytotoxic chromosomal targeting by CRISPR/Cas systems can reshape bacterial genomes and expel or remodel pathogenicity islands. *PLoS Genet* **9**, e1003454 (2013).

40. Musharova O*, et al.* Systematic analysis of type I-E *Escherichia coli* CRISPR-Cas PAM sequences ability to promote interference and primed adaptation. *Mol Microbiol* **111**, 1558-1570 (2019).

41. Blosser TR*, et al.* Two distinct DNA binding modes guide dual roles of a CRISPR-Cas protein complex. *Mol Cell* **58**, 60-70 (2015).

42. Redding S*, et al.* Surveillance and processing of foreign DNA by the *Escherichia coli* CRISPR-Cas system. *Cell* **163**, 854-865 (2015).

43. Xiao Y, Luo M, Dolan AE, Liao M, Ke A. Structure basis for RNA-guided DNA degradation by Cascade and Cas3. *Science* **361**, eaat0839 (2018).

44. van Erp PB, Jackson RN, Carter J, Golden SM, Bailey S, Wiedenheft B. Mechanism of CRISPR-RNA guided recognition of DNA targets in *Escherichia coli*. *Nucleic Acids Res* **43**, 8381-8391 (2015).

45. Nunez JK, Lee AS, Engelman A, Doudna JA. Integrase-mediated spacer acquisition during CRISPR-Cas adaptive immunity. *Nature* **519**, 193-198 (2015).

46. Jackson RN*, et al.* Crystal structure of the CRISPR RNA-guided surveillance complex from *Escherichia coli*. *Science* **345**, 1473-1479 (2014).

47. Sinkunas T, Gasiunas G, Fremaux C, Barrangou R, Horvath P, Siksnys V. Cas3 is a single-stranded DNA nuclease and ATP-dependent helicase in the CRISPR/Cas immune system. *EMBO J* **30**, 1335-1342 (2011).

48. Semenova E*, et al.* Interference by clustered regularly interspaced short palindromic repeat (CRISPR) RNA is governed by a seed sequence. *Proc Natl Acad Sci USA* **108**, 10098-10103 (2011).

49. Makarova KS, Zhang F, Koonin EV. SnapShot: Class 1 CRISPR-Cas Systems. *Cell* **168**, 946-946 (2017).

50. Patterson AG, Chang JT, Taylor C, Fineran PC. Regulation of the type I-F CRISPR-Cas system by CRP-cAMP and GalM controls spacer acquisition and interference. *Nucleic Acids Res* **43**, 6038-6048 (2015).

51. Malone LM, Hampton HG, Morgan XC, Fineran Peter C. Type I CRISPR-Cas provides robust immunity but incomplete attenuation of phage-induced cellular stress. *Nucleic Acids Res* **50**, 160-174 (2021).

52. Patterson AG*, et al.* Quorum sensing controls adaptive immunity through the regulation of multiple CRISPR-Cas systems. *Mol Cell* **64**, 1102-1108 (2016).

53. Staals RH, Jackson SA, Biswas A, Brouns SJ, Brown CM, Fineran PC. Interference-driven spacer acquisition is dominant over naive and primed adaptation in a native CRISPR-Cas system. *Nat Commun* **7**, 12853 (2016).

54. Campa Aroa R*, et al.* The Rsm (Csr) post-transcriptional regulatory pathway coordinately controls multiple CRISPR–Cas immune systems. *Nucleic Acids Res* **49**, 9508-9525 (2021).

55. Li M*, et al.* Toxin-antitoxin RNA pairs safeguard CRISPR-Cas systems. *Science* **372**, eabe5601 (2021).

56. Gong L, Li M, Cheng F, Zhao D, Chen Y, Xiang H. Primed adaptation tolerates extensive structural and size variations of the CRISPR RNA guide in *Haloarcula hispanica*. *Nucleic Acids Res* **47**, 5880-5891 (2019).

57. Li M, Wang R, Zhao D, Xiang H. Adaptation of the *Haloarcula hispanica* CRISPR-Cas system to a purified virus strictly requires a priming process. *Nucleic Acids Res* **42**, 2483-2492 (2013).

58. Xue C*, et al.* CRISPR interference and priming varies with individual spacer sequences. *Nucleic Acids Res* **43**, 10831-10847 (2015).

59. Høyland-Kroghsbo NM*, et al.* Quorum sensing controls the *Pseudomonas aeruginosa* CRISPR-Cas adaptive immune system. *Proc Natl Acad Sci USA* **114**, 131-135 (2017).

60. Westra ER*, et al.* H-NS-mediated repression of CRISPR-based immunity in *Escherichia coli* K12 can be relieved by the transcription activator LeuO. *Mol Microbiol* **77**, 1380-1393 (2010).

61. Fragel SM, Montada A, Heermann R, Baumann U, Schacherl M, Schnetz K. Characterization of the pleiotropic LysR-type transcription regulator LeuO of *Escherichia coli*. *Nucleic Acids Res* **47**, 7363-7379 (2019).

62. Pul U, Wurm R, Arslan Z, Geissen R, Hofmann N, Wagner R. Identification and characterization of *E. coli* CRISPR-*cas* promoters and their silencing by H-NS. *Mol Microbiol* **75**, 1495-1512 (2010).

63. Mitic D, Radovcic M, Markulin D, Ivancic-Bace I. StpA represses CRISPR-Cas immunity in H-NS deficient *Escherichia coli*. *Biochimie* **174**, 136-143 (2020).

64. Sun D, Mao X, Fei M, Chen Z, Zhu T, Qiu J. Histone-like nucleoid-structuring protein (H-NS) paralogue StpA activates the Type I-E CRISPR-Cas system againstnatural transformation in *Escherichia coli*. *Appl Environ Microbiol* **86**, e00731-00720 (2020).

65. Yang CD, Chen YH, Huang HY, Huang HD, Tseng CP. CRP represses the CRISPR/Cas system in *Escherichia coli*: evidence that endogenous CRISPR spacers impede phage P1 replication. *Mol Microbiol* **92**, 1072-1091 (2014).

66. Fang FC, Rimsky S. New insights into transcriptional regulation by H-NS. *Curr Opin Microbiol* **11**, 113-120 (2008).

67. Curran TD, Abacha F, Hibberd SP, Rolfe MD, Lacey MM, Green J. Identification of new members of the *Escherichia coli* K-12 MG1655 SlyA regulon. *Microbiology (Reading)* **163**, 400-409 (2017).

68. Nguyen Le Minh P, Velázquez Ruiz C, Vandermeeren S, Abwoyo P, Bervoets I, Charlier D. Differential protein-DNA contacts for activation and repression by ArgP, a LysR-type (LTTR) transcriptional regulator in *Escherichia coli*. *Microbiol Res* **206**, 141-158 (2018).

69. Lehnen D, Blumer C, Polen T, Wackwitz B, Wendisch VF, Unden G. LrhA as a new transcriptional key regulator of flagella, motility and chemotaxis genes in *Escherichia coli*. *Mol Microbiol* **45**, 521-532 (2002).

70. Breddermann H, Schnetz K. Activation of *leuO* by LrhA in *Escherichia coli*. *Mol Microbiol* **104**, 664-676 (2017).

71. Russel M, Linderoth NA, Sali A. Filamentous phage assembly: variation on a protein export theme. *Gene* **192**, 23-32 (1997).

72. Kunne T*, et al.* Cas3-derived target DNA degradation fragments fuel primed CRISPR adaptation. *Mol Cell* **63**, 852-864 (2016).

73. Fineran PC*, et al.* Degenerate target sites mediate rapid primed CRISPR adaptation. *Proc Natl Acad Sci USA* **111**, E1629-1638 (2014).

74. Cooper LA, Stringer AM, Wade JT. Determining the Specificity of Cascade Binding, Interference, and Primed Adaptation In Vivo in the Escherichia coli Type I-E CRISPR-Cas System. *mBio* **9**, e02100-02117 (2018).

75. Yoganand KN, Sivathanu R, Nimkar S, Anand B. Asymmetric positioning of Cas1-2 complex and integration host factor-induced DNA bending guide the unidirectional homing of protospacer in CRISPR-Cas type I-E system. *Nucleic Acids Res* **45**, 367-381 (2017).

76. Smith LM, Hampton HG, Yevstigneyeva MS, Mahler M, Paquet ZSM, Fineran PC. CRISPR-Cas immunity is repressed by the LysR-type transcriptional regulator PigU. *Nucleic Acids Res* **52**, 755-768 (2024).

77. Medina-Aparicio L*, et al.* The CRISPR/Cas immune system is an operon regulated by LeuO, H-NS, and leucine-responsive regulatory protein in *Salmonella enterica* serovar Typhi. *J Bacteriol* **193**, 2396-2407 (2011).

78. Stratmann T, Pul Ü, Wurm R, Wagner R, Schnetz K. RcsB-BglJ activates the *Escherichia coli leuO* gene, encoding an H-NS antagonist and pleiotropic regulator of virulence determinants. *Mol Microbiol* **83**, 1109-1123 (2012).

79. Yamanaka Y, Aizawa SI, Yamamoto K. The *hdeD* gene represses the expression of flagellum biosynthesis via LrhA in *Escherichia coli* K-12. *J Bacteriol* **204**, e0042021 (2022).

80. Datsenko KA, Wanner BL. One-step inactivation of chromosomal genes in *Escherichia coli* K-12 using PCR products. *Proc Natl Acad Sci USA* **97**, 6640-6645 (2000).

81. Erijman A, Dantes A, Bernheim R, Shifman JM, Peleg Y. Transfer-PCR (TPCR): a highway for DNA cloning and protein engineering. *J Struct Biol* **175**, 171-177 (2011).

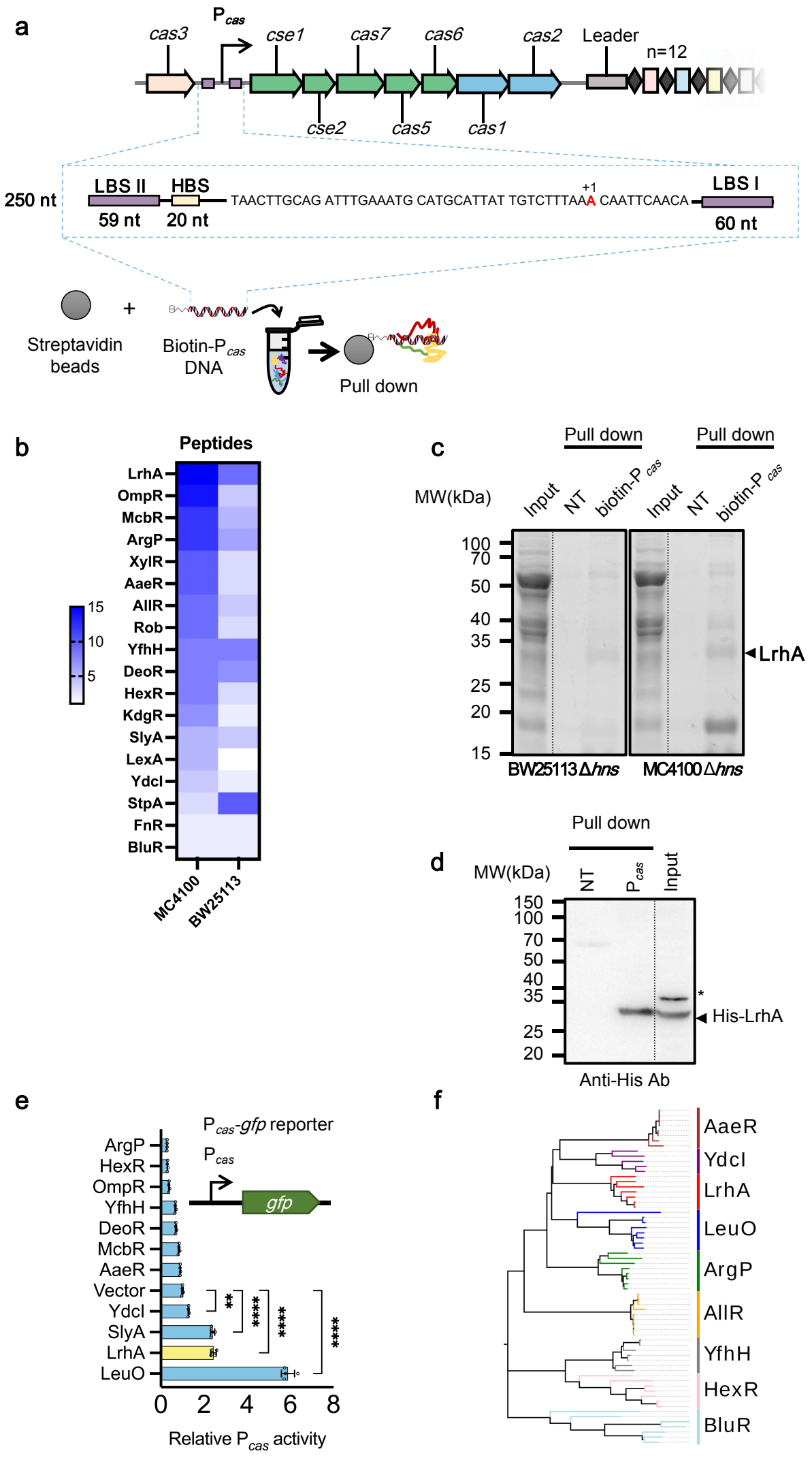
a
cas3
Pcas
cse1
cas7
cas6
cas2
Leader
n=12
cse2
cas5
cas1
250 nt
LBS II
HBS
TAACTTGCAG ATTTGAAATG CATGCATTAT TGTCTTTAAA CAATTCAACA
+1
LBS I
59 nt
20 nt
60 nt
Streptavidin beads
Biotin-Pcas DNA
Pull down
b
Peptides
LrhA
OmpR
McbR
ArgP
XylR
AaeR
AllR
Rob
YfhH
DeoR
HexR
KdgR
SlyA
LexA
YdcI
StpA
FnR
BluR
15
10
5
MC4100
BW25113
c
Pull down
Pull down
MW(kDa)
Input
NT
biotin-Pcas
Input
NT
biotin-Pcas
100
70
50
40
35
25
20
15
LrhA
BW25113Δhns
MC4100Δhns
d
Pull down
MW(kDa)
NT
Pcas
Input
150
100
70
50
40
35
25
20
*
His-LrhA
Anti-His Ab
e
Pcas-gfp reporter
Pcas
gfp
ArgP
HexR
OmpR
YfhH
DeoR
McbR
AaeR
Vector
YdcI
SlyA
LrhA
LeuO
**
****
****
****
0
2
4
6
8
Relative Pcas activity
f
AaeR
YdcI
LrhA
LeuO
ArgP
AllR
YfhH
HexR
BluR

Figure 1

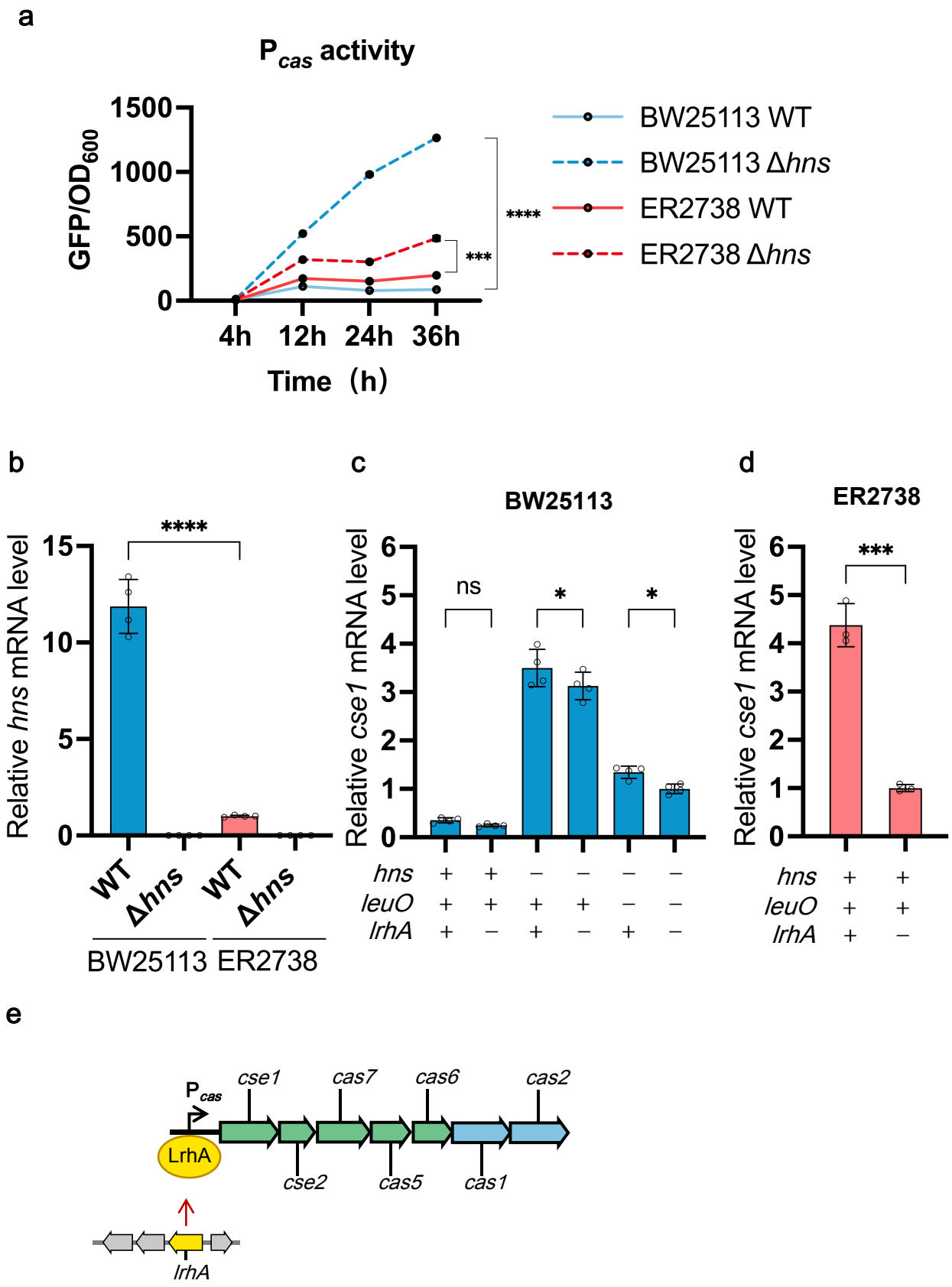
a
Pcas activity
GFP/OD600
1500
1000
500
0
4h
12h
24h
36h
Time (h)
****
***
BW25113 WT
BW25113 Δhns
ER2738 WT
ER2738 Δhns
b
Relative hns mRNA level
****
WT
Δhns
WT
Δhns
BW25113
ER2738
c
BW25113
Relative cse1 mRNA level
ns
*
*
hns
leuO
lrhA
d
ER2738
Relative cse1 mRNA level
***
hns
leuO
lrhA
e
Pcas
cse1
cas7
cas6
cas2
LrhA
cse2
cas5
cas1
lrhA

Figure 2

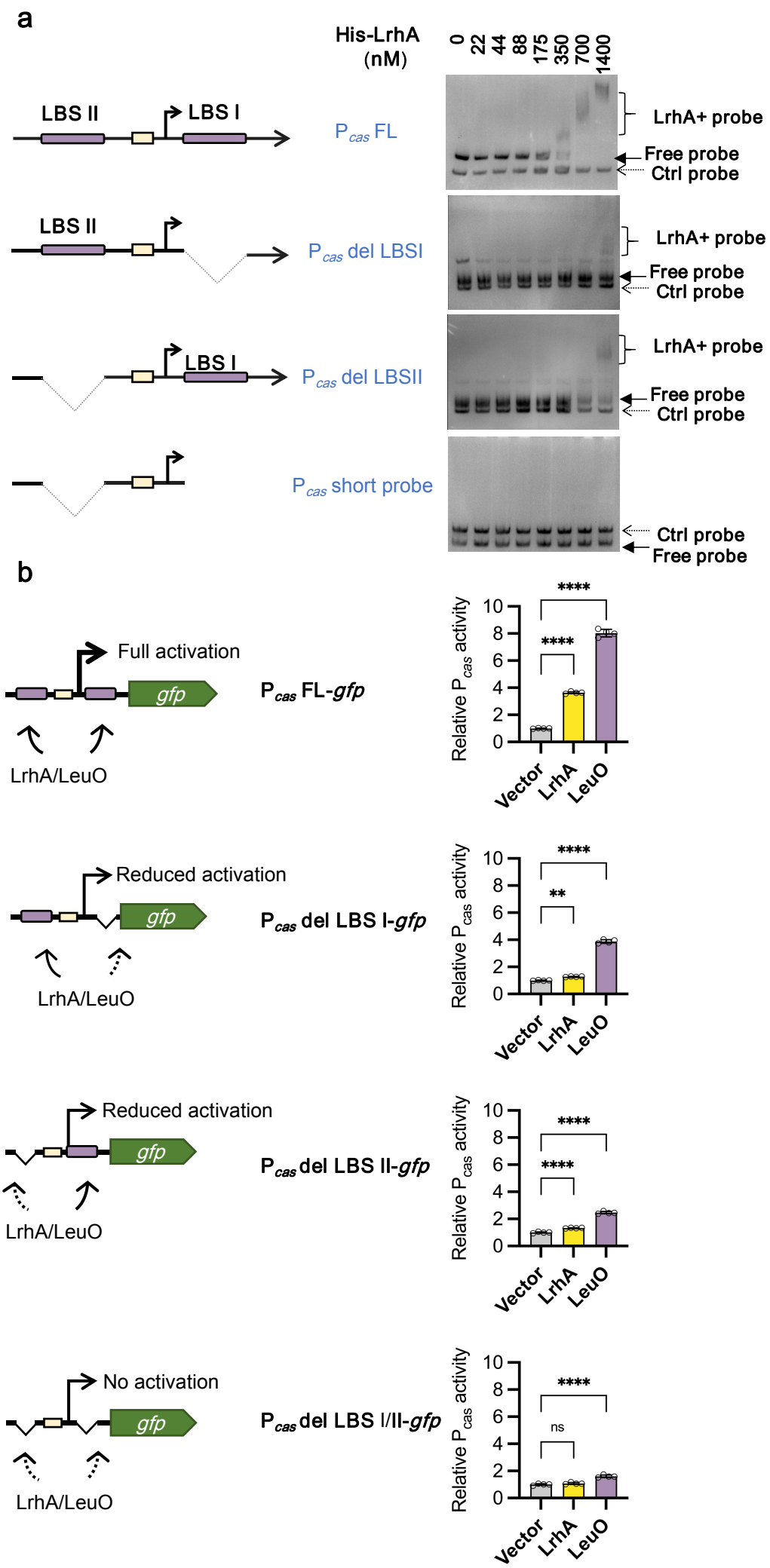
a
His-LrhA (nM)
0
22
44
88
175
350
700
1400
LBS II
LBS I
P cas FL
LrhA+ probe
Free probe
Ctrl probe
P cas del LBSI
P cas del LBSII
P cas short probe
b
Full activation
gfp
LrhA/LeuO
P cas FL-gfp
Relative P cas activity
Vector
LrhA
LeuO
Reduced activation
P cas del LBS I-gfp
P cas del LBS II-gfp
No activation
P cas del LBS I/II-gfp
ns

Figure 3

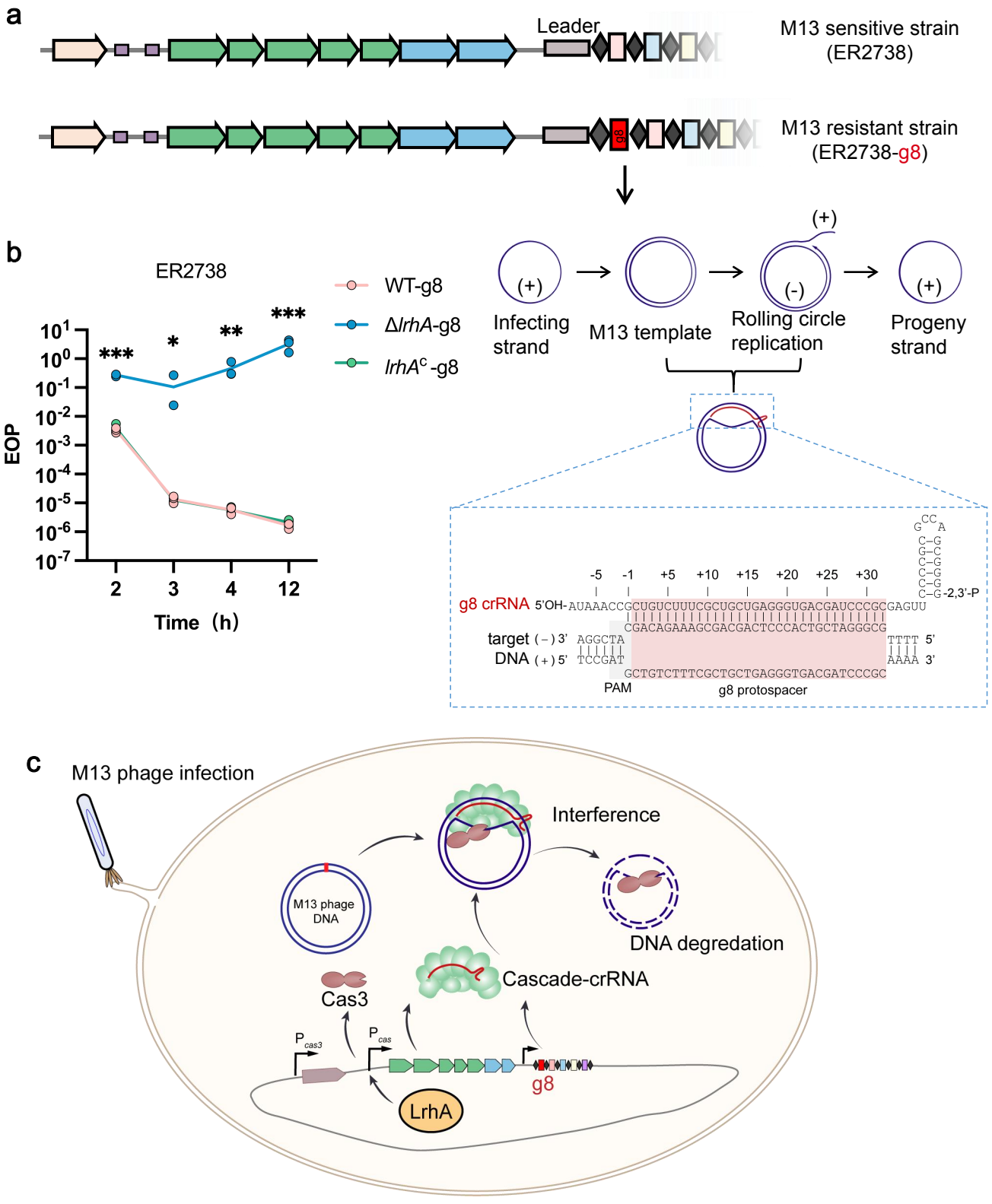
a
Leader
M13 sensitive strain
(ER2738)
g8
M13 resistant strain
(ER2738-g8)
b
ER2738
WT-g8
ΔlrhA-g8
lrhA^C-g8
EOP
Time (h)
Infecting strand
M13 template
Rolling circle replication
Progeny strand
(+)
(-)
g8 crRNA 5'OH-AUAAACCGCUGUCUUUCGCUGCUGAGGGUGACGAUCCCGCGAGUU
-2,3'-P
target (-)3' AGGCTA
DNA (+)5' TCCGAT
TTTT 5'
AAAA 3'
CGACAGAAAGCGACGACTCCCACTGCTAGGGCG
GCTGTCTTTCGCTGCTGAGGGTGACGATCCCGC
PAM
g8 protospacer
c
M13 phage infection
Interference
M13 phage DNA
DNA degredation
Cas3
Cascade-crRNA
g8
LrhA

Figure 4

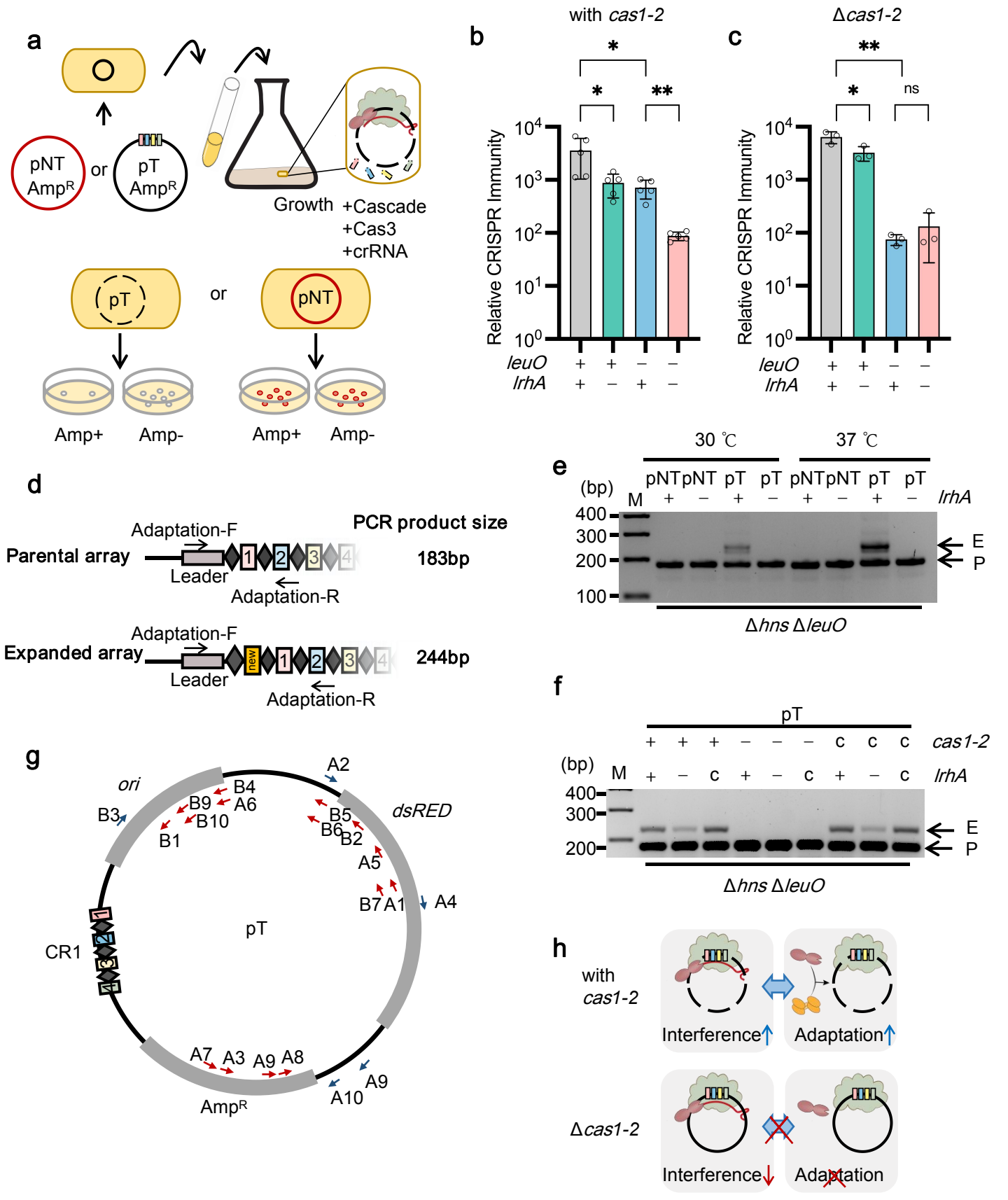
a
pNT
AmpR
or
pT
AmpR
Growth
+Cascade
+Cas3
+crRNA
pT
or
pNT
Amp+
Amp-
Amp+
Amp-
b
with cas1-2
Relative CRISPR Immunity
leuO
lrhA
c
Δcas1-2
ns
d
PCR product size
Parental array
Adaptation-F
Leader
Adaptation-R
183bp
Expanded array
new
244bp
e
30 ℃
37 ℃
(bp)
M
lrhA
E
P
Δhns ΔleuO
f
pT
cas1-2
lrhA
E
P
Δhns ΔleuO
g
ori
dsRED
pT
CR1
AmpR
h
with
cas1-2
Interference
Adaptation
Δcas1-2
Interference
Adaptation

Figure 5